Alteration of Sediments by Hyperalkaline K-Rich Cement Leachate: Implications for Strontium Adsorption and Incorporation

Sarah H. Wallace[1], Samuel Shaw[1,2], Katherine Morris[2], Joe S. Small[3] and Ian T. Burke[1]*

[1]Earth Surface Science Institute, School of Earth and Environment, University of Leeds, Leeds, LS2 9JT, UK. *Corresponding Author's E-mail: I.T.Burke@leeds.ac.uk; Phone: +44 113 3437532; Fax: +44 113 3435259

[2] Research Centre for Radwaste and Decommissioning and Williamson Research Centre, School of Earth, Atmospheric and Environmental Sciences, University of Manchester, Manchester, M13 9PL, U.K.

[3] National Nuclear Laboratory, Risley, Warrington, Cheshire, WA3 6AE, U.K.

Prepared for *Environmental Science and Technology*, 20 March 2013

ABSTRACT

Results are presented from one year batch experiments where K-rich hyperalkaline pH 13.5 young cement water (YCW) was reacted with sediments to investigate the effect of high pH, mineral alteration and secondary mineral precipitation on ^{90}Sr sorption. After reaction with YCW, Sr sorption was found to be >75 % in all samples up to 365 days, and 98 % in a sample reacted for 365 days at 70 °C. SEM analysis of sediment samples reacted at room temperature showed surface alteration and precipitation of a secondary phase, likely a K-rich aluminosilicate gel. The presence of Sr-Si(Al) bond distances in Sr K-edge EXAFS analysis suggested that the Sr was present as an inner-sphere adsorption complex. Sequential extractions, however, found the majority of this Sr was still exchangeable with Mg^{2+} at pH 7. For the sample reacted for one year at 70 °C, EXAFS analysis revealed clear evidence for ~6 Sr-Si(Al) backscatters at 3.45 Å, consistent with Sr incorporation into the neoformed K-chabazite phase that was detected by XRD and electron microscopy. Once incorporated into chabazite, ^{90}Sr was not exchangeable with Mg^{2+} and chemical leaching with pH 1.5 HNO_3 was required to remobilise 60 % of the ^{90}Sr. These results indicate that in high pH cementitious leachate there is significantly enhanced Sr retention in sediments due to changes in the adsorption mechanism and incorporation into secondary silicate minerals. This suggests that Sr retention may be enhanced in this high pH zone and that the incorporation process may lead to irreversible exchange of the contaminant over extended time periods.

KEYWORDS: Strontium-90, contaminated sediments, alkaline alteration, strontium incorporation, EXAFS, E-SEM, cementitious environments, nuclear legacy, alkaline tank waste.

TOC/Abstract art

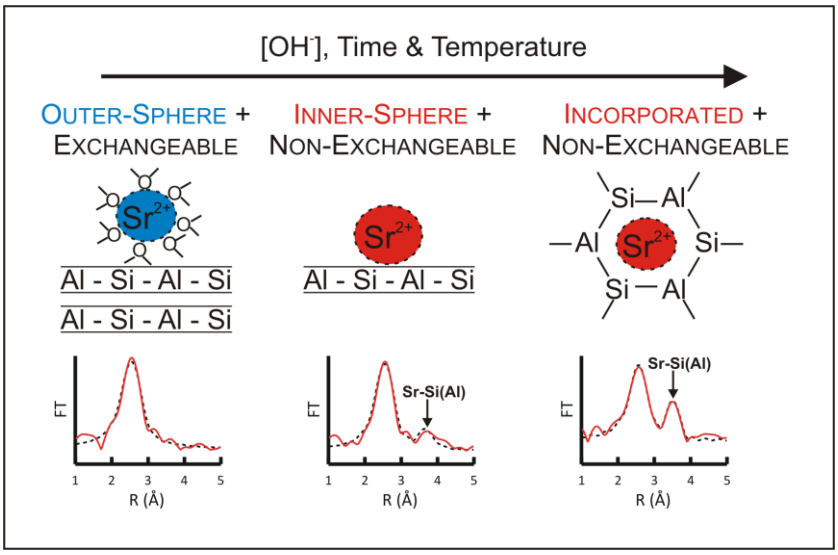

INTRODUCTION

The use of cementitious materials is ubiquitous at nuclear facilities around the world, where it is utilised in buildings, storage facilities and also the packaging of radioactive waste. When fresh cement and concrete comes into contact with water, a highly alkaline (0.3 – 0.7 mol L^{-1} OH^-) K- and Na-rich fluid forms, commonly known as young cement water (YCW) [1]. Interaction of such a hyperalkaline solution with aluminosilicate minerals in natural soils (e.g. clay minerals) and rock promotes the dissolution and recrystallisation of these minerals to neoformed phases (e.g. zeolites) [2-9]. These reactions lead to the formation of an alkaline disturbed zone in the geosphere surrounding the cement structures, which significantly alters the chemical (e.g. adsorption capacity) and physical (e.g. porosity) properties of the soils or sediment. This, in turn, could affect the mobility and speciation of radionuclides accidentally released into these environments. Therefore, understanding the processes occurring at the cement-geosphere interface and the effect of alkaline alteration on radionuclide speciation and mobility is key to the safe decommissioning of nuclear sites, some of which are considered the most hazardous facilities on the planet [10].

It is generally accepted that the reaction of aluminosilicate clay minerals (such as those found in bentonite) with alkaline fluids follows a two stage process: initial dissolution which releases Si and Al into solution, followed by precipitation/re-crystallisation of newly formed phases [3]. The exact reaction pathway and end product formed is highly dependent on the primary mineral (composition and structure), fluid composition and temperature [4, 11-14]. Studies of cement leachate interaction with bentonite barrier materials, which will be used in several national geodisposal repository programs [1, 8, 9, 15], indicates that these reactions lead to the formation of zeolites and/or calcium (aluminium) silicate hydrate (C-S-H) phases as reaction end points. Such phases have also been observed to occur at natural analogue sites where natural alkaline fluids (pH 12-13) react with silicate minerals in rocks [16, 17]. Studies of the mechanism of these secondary phase formation reactions from clays (e.g. kaolinite; bentonite), mixed with Na-rich fluids in model

systems, shows that the reaction proceeds via amorphous aluminosilicate and zeolite intermediate phases [12] with complete transformation to sodalite ($Na_8Cl_2[Al_6Si_6O_{24}]$) and cancrinite ($Na_6Ca_2[(CO_3)_2][Al_6Si_6O_{24}]\cdot 2H_2O$) phases at elevated temperatures or after very long reaction times [12]. However, the reaction of highly alkaline K-rich cement leachates with natural sediments/soils relevant to nuclear contaminated land, and the alteration pathways of clay minerals in these systems, has not been widely investigated.

Previous research of alkaline alteration of vadose zone sediments has focused on the interaction with highly caustic leak solutions, containing elevated concentrations of Na^+, NO_3^- and Al^{3+}, relevant to the US Department of Energy Hanford site [2, 3, 18-20]. Experimental studies conducted at a variety of temperatures have shown the formation of a wide range of secondary phases including zeolites, cancrinite and sodalite [21]. These minerals have framework structures with channels and cages which can accommodate both cations and anions [4]. Indeed, it has been demonstrated that both Sr^{2+} and Cs^+ can readily substitute into cancrinite and sodalite during alkaline alteration, and once incorporated, are relatively resistant to further remobilisation [19, 22]. It has, therefore, been proposed that this mechanism could be exploited for the retardation of contaminant radionuclides such as ^{90}Sr and ^{137}Cs under alkaline conditions [23]. However, the composition of cement leachate (i.e. dominated by K^+, Na^+, Ca^{2+}) is different to Hanford tank compositions, and therefore, a different reaction pathway may be expected. Clearly this is highly relevant to some legacy sites where accidentally released ^{90}Sr bearing fluids will have passed through and reacted with cementitious materials, prior to release into the surface soils and sediments.

This study, therefore, had the following objectives: 1) Investigate the nature of the mineral alteration reactions produced by highly alkaline cementitious leachate in contact with chlorite containing sediments (relevant to the UK Sellafield nuclear site) during incubation over long timescales (one year); 2) use X-ray absorption spectroscopy (XAS) to determine the nature of Sr^{2+}

incorporation occurring within secondary mineral precipitates, and sequential extractions to assess exchangeability and potential mobility of Sr^{2+} associated with these phases; 3) use the data produced to infer the likely importance of alkaline alteration of sediments in cementitious environments with respect to radionuclide mobility.

MATERIALS AND METHODS

Sediment Collection and Characterisation Unconsolidated sediments representative of the Sellafield nuclear facility in North West England were collected in August 2009 (Lat 54°26.3'N, Long 3°28.2'W). The sediment was dried at 40°C and sieved to retain the less than 2 mm fraction. Sediment characteristics are described in [24-26]. Briefly, the sediment was a fine grained silty sand (3 ± 1 % clay). The mineralogy was dominated by quartz (SiO_2) and feldspars (e.g. $(K,Na)AlSi_3O_8$). Chlorite ($Mg_5Al(AlSi_3)O_{10}(OH)_8$) was the dominant clay mineral with minor amounts of illite ($(K,H_3O)(Al,Mg,Fe)_2(Si,Al)_4O_{10}(OH)_2$) also detected. The sediment contained ~0.5 % organic carbon. SEM analysis revealed that the sediment contained angular and sub-angular quartz, feldspar and silicate rock fragments (mean grain size = 0.25 mm) coated in fine grained clay and iron oxide particles. The natural Sr content was 56 mg Kg^{-1}, which was non-exchangeably associated with minerals.

Batch Sorption Experiments Young cement water (YCW, pH 13.5) was made as follows: 25 ml saturated $Ca(OH)_2$ solution, 2.173 g Na_2SO_4, 2.876 g NaOH, 19.86 g KOH in 1 L deoxygenated DIW (saturated $Ca(OH)_2$ solution was made by placing 20 g $Ca(OH)_2$ in a dialysis bag and equilibrated for 120 days in 1 L deoxygenated DIW; pH 12.7). Dried sediment was weighed into 50 ml polypropylene Oak Ridge tubes and mixed with the YCW solution containing 20 mg L^{-1} Sr^{2+} (as $SrCl_2$) at a solid : solution ratio of 20 g L^{-1}, in an anaerobic chamber (97 % N_2 : 3% H_2; Coy Ltd, CA). All tubes were stored, in the dark, at 21 °C, inside airtight jars containing Carbosorb™ to remove atmospheric CO_2 for up to a year (carbonate would not form in the center of an alkaline subsurface plume, therefore,

CO_2 was excluded to avoid carbonate formation in experiments). Triplicate tubes were sacrificially sampled at 2, 10, 30, 90, 180 and 365 days. One set of triplicate tubes was stored in the dark at 70 °C for one year (hereafter referred to as '365 days +70 °C'). In addition, a duplicate set of three tubes for each time point were spiked with 30 Bq ml^{-1} ^{90}Sr tracer (6.5 x 10^{-11} mol L^{-1} as $SrCl_2$ in 0.01 mol L^{-1} HCl; CERCA-LEA, France) under argon, for aqueous geochemistry and sequential extraction measurements. At each sampling point, tubes were centrifuged at 6000 *g* for 10 minutes and the supernatant removed. The pH was determined in the aqueous phase using an Orion bench top meter, and major element concentrations determined on a Perkin Elmer 5300DV ICP-OES. Moist sediments from non-active tubes were stored at -80°C prior to X-ray absorption spectroscopy (XAS) analysis. Mineralogical components and the physical characteristics of the sediments were determined by XRD, BET and electron microscopy (see SI Section 1 for details).

Sequential Extractions Sequential extractions were carried out on tubes containing ^{90}Sr at each time point following an adapted Tessier/BCR method [27, 28] (see SI Table S1 for further details). The tubes were spun at 6000 *g* for 10 minutes, and the porewater removed and filtered (0.2 µm). The sediment was then progressively leached with 1 mol L^{-1} $MgCl_2$ (pH 7, 2 hours), 1 mol L^{-1} sodium acetate (pH 5, 5 hours) and finally 0.5 mol L^{-1} acidic hydroxylammonium chloride (pH 1.5, 12 hours). Between each stage the tubes were centrifuged and the supernatant removed and filtered as before and 1 ml of each extraction leachate was analysed for ^{90}Sr by liquid scintillation counting (LSC) on a Parkard Tri-Carb 2100TR (see SI Section 2 for details).

X-ray Absorption Spectroscopy (XAS) Sr K-edge (16,105 eV) XAS spectra were collected at beamline BM26A at the European Synchrotron Radiation Facility in January 2011. Approximately 300 mg of moist sediment samples (10 day, 365 day and 365 day + 70°C) were prepared under argon atmosphere in aluminium holders with Kapton™ windows and data were collected at 80 °K using a liquid nitrogen cryostat. Spectra were also collected from a $SrCl_2$ solution (3000 mg L^{-1}) and $SrCO_3$ standards. Extended X-ray absorption fine edge structure (EXAFS) spectra were averaged using

Athena v0.8.061 and background subtracted using PySpline v1.1 [29]. EXAFS data were analysed in DLexcurv v1.0 [30] using full curved wave theory [31]. The data were fitted for each sample by defining a theoretical model and comparing the calculated EXAFS spectrum with experimental data. Shells of backscatterers were added around the Sr and by refining an energy correction Ef (the Fermi Energy), the absorber-scatterer distance, and the Debye-Waller factor for each shell; a least squares residual (the *R* factor [32]) was minimised. Shells or groups of shells were only included if the overall fit (*R*-factor) was reduced by > 5 % (see [33] and SI Section S3 for further details of beamline set-up and analysis protocols).

RESULTS

Solution Analysis and Sequential Extractions During reaction of the sediment with YCW the pH remained at 13.49 $\pm$ 0.29 in all experiments. The activity of ^{90}Sr tracer in solution (aqueous phase in Figure 1) decreased from 30 Bq ml^{-1} at the start of the 21°C reaction to 8.6 $\pm$ 2.7 Bq ml^{-1} after 2 days, decreasing to a minimum of 1.9 $\pm$ 1.0 Bq ml^{-1} after 10 days. During further aging the ^{90}Sr activity in solution gradually rose to reach 7.7 $\pm$ 3.6 Bq ml^{-1} at 365 days. In sequential extractions, the majority (70 - 80 %) of the ^{90}Sr activity associated with sediment was recovered in the $MgCl_2$ exchangeable fraction, with the remaining 20 - 30 % recovered in other fractions or residual. In the 365 days +70°C sample, only 0.6 $\pm$ 0.1 Bq ml^{-1} was found in solution with the majority (17.3 $\pm$ 1.8 Bq ml^{-1}; 60.2 $\pm$ 6.2 %) of the ^{90}Sr added recovered in the acidic hydroxylammonium chloride fraction and 24 $\pm$ 6 % was residual.

At 2 days, the [Si] and [Al] (714 $\pm$ 229 and 22 $\pm$ 8 mg L^{-1}) are elevated despite neither being added to the initial YCW composition (Figure 2). Thereafter, the [Si] and [Al] decrease at day 10, then remain at broadly similar levels from 10 – 365 days with an initial decrease to a minimum concentration of 16 $\pm$ 1 and 11 $\pm$ 1 mg L^{-1} at 30 days, and then a slow increase to 45 $\pm$ 10 and 43 $\pm$ 8 mg L^{-1} respectively by 365 days. In the 365 days +70°C sample [Si] is 949 $\pm$ 115 mg L^{-1} and [Al] is 2.6 $\pm$ 0.1 mg L^{-1}. Aqueous K and Na concentrations at 2 days were slightly below YCW composition, [K] =

11600 ± 700 mg L^{-1}, [Na] = 2000 ± 100 mg L^{-1} (vs. 13833 ± 1100 and 2350 ± 190 mg L^{-1} in YCW). K and Na concentrations reached a minimum value of 5800 ± 300 and 1100 ± 20 mg L^{-1} respectively at 30 days. K and Na concentrations then steadily increased to within error of the concentration reported from the 2 day sample in both the 365 days and the 365 days +70°C samples.

XRD, SEM, BET and Electron Microprobe Analysis XRD results (Figure 3) indicated that the bulk mineralogy of the sediments did not change during the reaction with YCW up to 365 days. However, qualitatively, the intensity of the chlorite peaks relative to the peaks of the bulk mineral phases (i.e. quartz and feldspar) was reduced in samples reacted with YCW compared to unreacted sediments, whereas the illite/muscovite peaks were unchanged. SEM analysis of the unreacted sediment (Figure 4a) revealed sand and silt sized quartz and feldspar grains coated with <5 μm aluminosilicate clay particles with a plate-like morphology. After 10 days reaction with YCW (Figure 4b) the clay particles were still visible as a surface coating on the grains, but their surface appeared altered, i.e. smoother. EDX analyses of the aluminosilicate clay particles (SI Figure S1) showed they contained elevated K compared to the material coating the unreacted sediments. After 365 days reaction (Figure 4c), the surfaces of the grains were coated with a smooth fine grained (i.e. nanoparticulate) secondary precipitate. EDX analyses revealed the precipitate had a similar K-rich aluminosilicate composition as was present at 10 days. Due to the thinness of the coating, the presence of other phases in the EDX excitation volume (~ 2 μm^3) could not be excluded, therefore, it was impossible to determine a reproducible EDX analysis of the coating.

In the 365 days +70 °C sample additional peaks were present in XRD patterns that were assigned to the zeolite mineral, chabazite. In contrast to sediments from reactions at room temperature, sediment grains in the 365 days +70 °C sample (Figure 4d) were coated in flattened 5-10 μm diameter disc-shaped crystals made up of smaller inter-grown crystallites. This morphology is similar to previous reports of newly formed chabazite [5]. SEM-EDX analysis of the new phases consisted of K-Na-Al-Si-O (SI Figure S1). Electron microprobe analysis of the individual particles (SI

Figure S2 and Table S2) yielded a chemical formula of $(K_{1.2}Na_{0.3}Sr_{0.1}Ca_{0.1})[Si_{2.5}Al_{3.6}O_{12}]\cdot 5.9H_20$ (SI Table S3) consistent with the idealised formula of K-chabazite, $(K_2Al_2Si_4O_{12})\cdot 6H_2O$ substituted with ~2 $\pm$ 1 wt % Sr. The BET surface area of the unreacted sediment was measured as 4.69 ± 0.01 m^2g^{-1}. After 10 days reaction, the surface area measured in the sample had decreased to 1.46 ± 0.02 $m^2\ g^{-1}$ (Table 1). Further time points in the experiments at 21 °C showed no significant change in surface area. In contrast, in the 365 +70 °C sample the surface area was 5.45 ± 0.03 $m^2\ g^{-1}$.

Sr-EXAFS Analysis Sr K-edge EXAFS data collected from sediment reacted with YCW for 10 days (Figure 5; Table 2) revealed a Sr coordination environment of ~8 O atoms at 2.59 Å. Data was fitted with one further shell containing ~3 Si(Al) backscatters at 3.79 Å (due to their similar atomic mass Si and Al are indistinguishable in EXAFS analysis). Data collected from the sample recovered after 365 days reaction also revealed a first shell coordination of ~8 O atoms at 2.60 Å and a second shell fitted with ~1 Si(Al) backscatter at 3.84 Å. In the 365 days +70°C sample the EXAFS data was best fit with a first shell containing ~8 O atoms at 2.67 Å and a single additional shell of ~6 Si(Al) backscatters at 3.45 Å.

DISCUSSION

Low Temperature (21 ^oC) Reaction of Sediments with YCW. Addition of alkaline fluids, such as K-rich YCW, to sediments induces a rapid (within 2 days) initial dissolution of the reactive, high surface area aluminosilicate clay within the sediment leading to a rapid increase in dissolved Si and Al [18]. Consistent with previous observations of alkaline sediment alteration [21], in these experiments XRD analysis suggests that chlorite appears to be the key reactive clay phase within the sediment. After 10 days reaction at room temperature, the observed surface alteration of the sediment grains, in conjunction with the rapid increase then decline in Si and Al solution concentration indicated that precipitation of a secondary phase had begun to occur (as observed in similar alkaline alteration experiments using Hanford sediments [34]). The K-Al-Si-rich composition

of this coating, lack of defined crystalline morphology and XRD peaks indicates it is either a K-rich aluminosilicate amorphous gel or nanocrystalline phases where the crystalline particles are too small to form distinct XRD peaks. However, at the temperature and duration of the experiments the formation of an amorphous gel is most plausible [5].

By 365 days reaction at room temperature, SEM indicated a large increase in the amount of the secondary aluminosilicate phase formed. Again the lack of any crystalline morphology and the absence of any additional peaks in the XRD pattern of the reaction products suggest the secondary phases has remained poorly ordered. A small increase in SSA_{BET} was observed (1.46 ±0.02 to 1.66 ±0.01 m^2g^{-1}) after 365 days reaction and was also attributed to the presence of increased amounts of the secondary phase. SEM-EDX analysis of the secondary phase at 365 days showed that it remained a K-rich aluminosilicate gel. This is consistent with other studies which show the formation of aluminosilicate gels from Si and Al rich solutions [5, 34]. Alkaline alteration of aluminosilicates commonly proceeds via dissolution and precipitation of amorphous gel phases that can then transform to more crystalline phases with time and temperature [7, 12]. At 21°C, however, the temperature was presumably too low to allow crystallisation.

The majority of the ^{90}Sr tracer added remained sorbed ('sorbed' or 'sorption' here refers to Sr removed from solution with no specific information regarding whether it is surface adsorbed or incorporated) to sediments throughout the 365 days of reaction with YCW (pH = 13.5) at room temperature (K_d = 180 and 700 L Kg^{-1} at 365 and 10 days respectively). This is in contrast to previous work using the same sediment [26], which showed that Sr adsorption decreases with pH above 8 due to the increase in ionic strength caused by the addition of Na^+ or Ca^{2+} ions and cation exchange of the outer-sphere adsorbed Sr ('adsorbed' or 'adsorption' here refers to Sr specifically associated with mineral surfaces). At a pH of 10 the adsorption of ^{90}Sr was low (K_d ~1 L Kg^{-1}), and if this trend were to continue it predicts that at pH 13.5 ^{90}Sr adsorption would be extremely low due to high ionic strength (>0.1 mol L^{-1} in YCW). Interestingly, our data contradicts this prediction indicating that Sr is

sorbed to the mineral particles via a different mechanism than that at lower pH (e.g. pH ≤ 10). Sr K-edge EXAFS spectra collected from samples recovered at 10 and 365 days (Figure 5) did not indicate that the Sr was present as a simple outer sphere adsorption complex, due to the presence of Si(Al) atoms at bond distance ≈ 3.8 Å. This is consistent with Sr-Si(Al) bond distances observed in previous alkaline alteration experiments using natural sediments which were attributed to inner-sphere adsorption to secondary aluminosilicate phases [19]. Therefore we suggest that the high levels of sorption at pH 13.5 observed in these experiments was due inner-sphere adsorption of Sr associated with the secondary K-rich aluminosilicate precipitate or altered clay minerals (Figure 4d).

This interpretation explains the large difference in adsorption observed at pH 10 [26] relative to pH 13.5 in this study, as our data suggest there is a fundamental change in the adsorption mechanism which then dramatically increases adsorption. This is because unlike outer-sphere adsorption, surface uptake during inner-sphere adsorption is not affected by ionic strength [35]. However, it should be noted that in our experiments a high proportion of the ^{90}Sr was exchanged from the sediments using a pH 7 $MgCl_2$ extraction. The apparent selectivity of Sr^{2+} to exchange with Mg^{2+} rather than Na^+ or K^+ in the YCW solution was attributed to a change in adsorption mechanism when the alkaline reacted materials were reacted with a pH 7, 1 mol L^{-1}, $MgCl_2$ solution. The direct addition of the solution to reacted sediments resulted in a substantial decrease in pH, changing the Sr adsorption to an outer-sphere mechanism which is susceptible to exchange by Mg^{2+}. We suggest that this observation shows that the change in Sr adsorption mechanism is not due to the alteration of the silicate minerals by the alkaline fluid, but is simply a function of the high pH.

High Temperature (70 ^{o}C) Reaction of Sediments with YCW Reaction of the sediment with K-rich YCW for 365 days at 70°C produced a new crystalline phase. A combination of morphological, XRD and microprobe data provides strong evidence that K-chabazite (zeolite) was the stable endpoint of alkaline alteration. The formation of K-chabazite has also been observed in reactions of bentonite and KOH dominated alkaline solutions at similar pH and temperature (pH 13.5, 60°C) [5].

The crystalline end-product formed is often controlled by the composition of the alkaline fluid. For example, the reaction of bentonite with NaOH solution (pH > 12.9), produces Na-rich analcime ($NaAlSi_2O_6 \cdot H_2O$) [15] whereas alteration of sediments with Na, Al and nitrate rich fluids (pH > 13) (such as those found at the US Hanford site) more commonly forms feldspathoids such as sodalite and cancrinite [19, 36].

In the 365 day +70 °C sample, very high ^{90}Sr K_d values were observed (~ 2500 L Kg^{-1}) indicating that formation of chabazite promoted much higher levels of Sr sorption than the room temperature reaction. Sr K-edge EXAFS spectra collected from reference chabazite show a characteristic elongated 1st shell Sr-O bond distance at 2.67 Å (compared to more usual Sr-O distance of ~2.60 Å found where Sr is present in a hydration sphere) and strong second shell Sr-Si(Al) scattering at 3.45 Å [21]. The EXAFS spectra collected from the 365 day +70 °C sample had a similar elongation of the first shell Sr-O bond distance (2.67 Å) and also featured a strong second shell of ~6 Sr-Si(Al) backscatterers at a distance of 3.45 Å, consistent with incorporation of Sr into the neoformed chabazite. These bond distances are correct for incorporation of Sr^{2+} into the aluminosilicate cage within the chabazite structure below the D6R ring (cation site 1 in [37]). Sequential extraction results demonstrated that ^{90}Sr incorporated in this site is non-exchangeable with Mg^{2+}, primarily due to the small diameter cage entrance compared with the hydrated Sr^{2+} ionic radius (~ 3.8 Å for the cage entrance vs. ~ 5.2 Å for hydrated Sr^{2+}) [38-40]. Once incorporated, Sr^{2+} is therefore recalcitrant to extraction by ion exchange and re-release requires dissolution of the hosting mineral [19, 22]. Our sequential extraction results showed the majority of the ^{90}Sr tracer was recovered during acidic hydroxylammonium chloride (pH 1.5) leaching of the sample. Several chabazite phases are indeed reported to unstable below ~pH 2 [41, 42], therefore, we ascribe this behaviour to chabazite dissolution by the acidic lixivant.

Implications for Cementitious Environments. Alkaline alteration of minerals by reaction with K-rich YCW solution will result in enhanced sorption potential with respect to cationic species

such as Sr^{2+} either through increased adsorption to altered clay minerals and secondary intermediates or potential incorporation into newly formed phases [19, 21]. At low temperatures (20-40 ^{o}C) K-chabazite supersaturation is predicted throughout the high pH reactions (SI Tables S4 and S5) studied here (the K-feldspathiod mineral, leucite ($KAlSi_2O_6$) was also predicted to be oversaturated; however, the degree of oversaturation was considerably lower than that of chabazite), but no crystalline phases form and instead an aluminosilicate gel occurred [5]. This is primarily due to the low temperature, and high activation energies of crystallisation (e.g. > 65 kJ mol^{-1} for zeolites [43]) which limit crystallisation rates to very low levels. However, when reaction temperatures are elevated above 60 ^{o}C, several different zeolite phases are observed in K-rich YCW systems [15], with K-chabazite the relevant phase at 60-70 ^{o}C [5]..

It is not known if the differences between the high and low temperature reaction end points simply reflect differences in crystallisation rates or differences in mineral stabilities meaning that zeolite phases will not form at lower temperatures. However, when considering the transport of ^{90}Sr, with a half-life of 29 years, even if zeolite phases were thermodynamically stable the kinetics of crystallisation may be slower than the few centuries required for ^{90}Sr to decay to safe levels. Although the behaviour of ^{90}Sr is not relevant to geological disposal, it is interesting to note the preferential YCW reactions with reactive clay phases observed in these experiments. This is relevant to deep disposal where the results of this study and others [19, 21, 23, 36] demonstrate it is reaction with clay mineral components of mineral assemblages that controls the development of solution chemistry and mineral surfaces.

In the systems without zeolite formation, the mineral surfaces present at high pH have a high sorption capacity for ^{90}Sr due to changes to an inner sphere adsorption mechanism in solutions with pH > 12-13. This indicates that very high pH (>12-13) will limit ^{90}Sr transport at contaminated sites at all temperatures, where Sr can be susceptible to cation exchange by higher ionic strength

(>10 mmols L^{-1}) waters [26]. It also suggests that any ^{90}Sr associated with cement or concrete will not migrate a significant distance due to the highly alkaline nature of the cement pore fluids.

ACKNOWLEDGEMENTS

The authors acknowledge funding from the UK Engineering and Physical Science Research Council and the UK Nuclear Decommissioning Authority (Award 07000878). The European Synchrotron Radiation Facility is thanked for access to beamline BM26a (Grant EC-740), and we acknowledge support from UK Natural Environment Research Council Grant NE/H007768/1. We thank Rachel Gasior, Lesley Neve and Richard Walshaw (University of Leeds) and Clare Thorpe (University of Manchester) for assistance with ICP-OES, XRD, electron microscopy and XAS analysis respectively.

Supporting Information. Detailed aqueous sampling and analysis methods, XAS methods, solid analysis methods, electron microprobe images and tabulated data, solution composition and mineral saturation modelling results, SEM-EDX spectra. This material is available free of charge via the Internet at http://pubs.acs.org.

REFERENCES

1. Fernandez, R.; Mader, U. K.; Rodriguez, M.; de la Villa, R. V.; Cuevas, J., Alteration of compacted bentonite by diffusion of highly alkaline solutions. *European Journal of Mineralogy* **2009,** *21*, (4), 725-735.
2. Bickmore, B. R.; Nagy, K. L.; Young, J. S.; Drexler, J. W., Nitrate-cancrinite precipitation on quartz sand in simulated Hanford tank solutions. *Environmental Science & Technology* **2001,** *35*, (22), 4481-4486.
3. Zhao, H. T.; Deng, Y. J.; Harsh, J. B.; Flury, M.; Boyle, J. S., Alteration of kaolinite to cancrinite and sodalite by simulated hanford tank waste and its impact on cesium retention. *Clays and Clay Minerals* **2004,** *52*, (1), 1-13.
4. Deng, Y. J.; Harsh, J. B.; Flury, M.; Young, J. S.; Boyle, J. S., Mineral formation during simulated leaks of Hanford waste tanks. *Applied Geochemistry* **2006,** *21*, (8), 1392-1409.
5. Fernandez, R.; Rodriguez, M.; de la Villa, R. V.; Cuevas, J., Geochemical constraints on the stability of zeolites and C-S-H in the high pH reaction of bentonite. *Geochimica et Cosmochimica Acta* **2010,** *74*, (3), 890-906.
6. Khoury, H. N.; Salameh, E.; Clark, I. D.; Fritz, P.; Bajjali, W.; Milodowski, A. E.; Cave, M. R.; Alexander, W. R., A natural analogue of high pH cement pore waters from the Maqarin area of northern Jordan. I: introduction to the site. *Journal of Geochemical Exploration* **1992,** *46*, (1), 117-132.
7. Savage, D.; Walker, C.; Arthur, R.; Rochelle, C.; Oda, C.; Takase, H., Alteration of bentonite by hyperalkaline fluids: A review of the role of secondary minerals. *Physics and Chemistry of the Earth, Parts A/B/C* **2007,** *32*, (1–7), 287-297.
8. Ramírez, S.; Cuevas, J.; Vigil, R.; Leguey, S., Hydrothermal alteration of "La Serrata" bentonite (Almeria, Spain) by alkaline solutions. *Applied Clay Science* **2002,** *21*, (5–6), 257-269.
9. Nakayama, S.; Sakamoto, Y.; Yamaguchi, T.; Akai, M.; Tanaka, T.; Sato, T.; Iida, Y., Dissolution of montmorillonite in compacted bentonite by highly alkaline aqueous solutions and diffusivity of hydroxide ions. *Applied Clay Science* **2004,** *27*, (1–2), 53-65.
10. McKie, R., Sellafield: the most hazardous place in Europe. *The Observer [online]. 19 April 2009 [Accessed 26 November 2012]. Available from: http://www.guardian.co.uk/environment/2009/apr/19/sellafield-nuclear-plant-cumbria-hazards* 2009.
11. Barnes, M. C.; Addai-Mensah, J.; Gerson, A. R., The mechanism of the sodalite-to-cancrinite phase transformation in synthetic spent Bayer liquor. *Microporous and Mesoporous Materials* **1999,** *31*, (3), 287-302.
12. Deng, Y. J.; Flury, M.; Harsh, J. B.; Felmy, A. R.; Qafoku, O., Cancrinite and sodalite formation in the presence of cesium, potassium, magnesium, calcium and strontium in Hanford tank waste simulants. *Applied Geochemistry* **2006,** *21*, (12), 2049-2063.
13. Huang, W. L., THE FORMATION OF ILLITIC CLAYS FROM KAOLINITE IN KOH SOLUTION FROM 225-DEGREES-C TO 350-DEGREES-C. *Clays and Clay Minerals* **1993,** *41*, (6), 645-654.
14. Heller-Kallai, L.; Lapides, I., Reactions of kaolinites and metakaolinites with NaOH - comparison of different samples (Part 1). *Applied Clay Science* **2007,** *35*, (1-2), 99-107.
15. Sanchez, L.; Cuevas, J.; Ramirez, S.; De Leon, D. R.; Fernandez, R.; Dela Villa, R. V.; Leguey, S., Reaction kinetics of FEBEX bentonite in hyperalkaline conditions resembling the cement-bentonite interface. *Applied Clay Science* **2006,** *33*, (2), 125-141.
16. Savage, D., A review of analogues of alkaline alteration with regard to long-term barrier performance. *Mineralogical Magazine* **2011,** *75*, (4), 2401-2418.
17. Gaucher, E. C.; Blanc, P., Cement/clay interactions – A review: Experiments, natural analogues, and modeling. *Waste Management* **2006,** *26*, (7), 776-788.

18. Chorover, J.; Choi, S. K.; Amistadi, M. K.; Karthikeyan, K. G.; Crosson, G.; Mueller, K. T., Linking cesium and strontium uptake to kaolinite weathering in simulated tank waste leachate. *Environmental Science & Technology* **2003,** *37*, (10), 2200-2208.
19. Chorover, J.; Choi, S.; Rotenberg, P.; Serne, R. J.; Rivera, N.; Strepka, C.; Thompson, A.; Mueller, K. T.; O'Day, P. A., Silicon control of strontium and cesium partitioning in hydroxide-weathered sediments. *Geochimica Et Cosmochimica Acta* **2008,** *72*, (8), 2024-2047.
20. Rod, K. A.; Um, W.; Flury, M., Transport of Strontium and Cesium in Simulated Hanford Tank Waste Leachate through Quartz Sand under Saturated and Unsaturated Flow. *Environmental Science & Technology* **2010,** *44*, (21), 8089-8094.
21. Perdrial, N.; Rivera, N.; Thompson, A.; O'Day, P. A.; Chorover, J., Trace contaminant concentration affects mineral transformation and pollutant fate in hydroxide-weathered Hanford sediments. *Journal of Hazardous Materials* **2011,** *197*, (0), 119-127.
22. Choi, S.; O'Day, P. A.; Rivera, N. A.; Mueller, K. T.; Vairavamurthy, M. A.; Seraphin, S.; Chorover, J., Strontium speciation during reaction of kaolinite with simulated tank-waste leachate: Bulk and microfocused EXAFS analysis. *Environmental Science & Technology* **2006,** *40*, (8), 2608-2614.
23. Thompson, A.; Steefel, C. I.; Perdrial, N.; Chorover, J., Contaminant Desorption during Long-Term Leaching of Hydroxide-Weathered Hanford Sediments. *Environmental Science & Technology* **2010,** *44*, (6), 1992-1997.
24. Law, G. T. W.; Geissler, A.; Boothman, C.; Burke, I. T.; Livens, F. R.; Lloyd, J. R.; Morris, K., Role of Nitrate in Conditioning Aquifer Sediments for Technetium Bioreduction. *Environmental Science & Technology* **2010,** *44*, (1), 150-155.
25. Thorpe, C. L.; Lloyd, J. R.; Law, G. T. W.; Burke, I. T.; Shaw, S.; Bryan, N. D.; Morris, K., Strontium sorption and precipitation behaviour during bioreduction in nitrate impacted sediments. *Chemical Geology* **2012,** *306–307*, 114-122.
26. Wallace, S. H.; Shaw, S.; Morris, K.; Small, J. S.; Fuller, A. J.; Burke, I. T., Effect of groundwater pH and ionic strength on strontium sorption in aquifer sediments: Implications for 90Sr mobility at contaminated nuclear sites. *Applied Geochemistry* **2012,** *27*, (8), 1482-1491.
27. Tessier, A.; Campbell, P. G. C.; Bisson, M., Sequential Extraction Procedure for the Speciation of Particulate Trace-Metals. *Analytical Chemistry* **1979,** *51*, (7), 844-851.
28. Burke, I. T.; Livens, F. R.; Lloyd, J. R.; Brown, A. P.; Law, G. T. W.; McBeth, J. M.; Ellis, B. L.; Lawson, R. S.; Morris, K., The fate of technetium in reduced estuarine sediments: Combining direct and indirect analyses. *Applied Geochemistry* **2010,** *25*, (2), 233-241.
29. Tenderholt, A.; Hedman, B.; Hodgson, K. O., PySpline: A modern, cross-platform program for the processing of raw averaged XAS edge and EXAFS data. In *X-Ray Absorption Fine Structure-XAFS13*, Hedman, B. P. P., Ed. 2007; Vol. 882, pp 105-107.
30. Tomic, S.; Searle, B. G.; Wander, A.; Harrison, N. M.; Dent, A. J.; Mosselmans, J. F. W.; Inglesfield, J. E. *New Tools for the Analysis of EXAFS: The DL_EXCURV Package, CCLRC Technical Report DL-TR-2005-00, ISSN 1362-0207*; Daresbury SRS 2005: 2005.
31. Gurman, S. J.; Binsted, N.; Ross, I., A RAPID, EXACT CURVED-WAVE THEORY FOR EXAFS CALCULATIONS. *Journal of Physics C-Solid State Physics* **1984,** *17*, (1), 143-151.
32. Binsted, N.; Strange, R. W.; Hasnain, S. S., CONSTRAINED AND RESTRAINED REFINEMENT IN EXAFS DATA-ANALYSIS WITH CURVED WAVE THEORY. *Japanese Journal of Applied Physics Part 1-Regular Papers Short Notes & Review Papers* **1993,** *32*, 141-143.
33. Nikitenko, S.; Beale, A. M.; van der Eerden, A. M. J.; Jacques, S. D. M.; Leynaud, O.; O'Brien, M. G.; Detollenaere, D.; Kaptein, R.; Weckhuysen, B. M.; Bras, W., Implementation of a combined SAXS/WAXS/QEXAFS set-up for time-resolved in situ experiments. *Journal of Synchrotron Radiation* **2008,** *15*, 632-640.

34. Qafoku, N. P.; Ainsworth, C. C.; Szecsody, J. E.; Qafoku, O. S., Aluminum Effect on Dissolution and Precipitation under Hyperalkaline Conditions: I. Liquid Phase Transformations. *J. Environ. Qual.* **2003,** *32*, (6), 2354-2363.
35. Krauskopf, K. B., *Introduction to geochemistry / Konrad B. Krauskopf, Dennis K. Bird*. 3rd ed.; McGraw-Hill: New York, 1995.
36. Qafoku, N. P.; Ainsworth, C. C.; Szecsody, J. E.; Bish, D. L.; Young, J. S.; McCready, D. E.; Qafoku, O. S., Aluminum effect on dissolution and precipitation under hyperalkaline conditions: II. Solid phase transformations. *Journal of Environmental Quality* **2003,** *32*, (6), 2364-2372.
37. Calligaris, M.; Nardin, G.; Randaccio, L.; Chiaramonti, P. C., CATION-SITE LOCATION IN A NATURAL CHABAZITE. *Acta Crystallographica Section B-Structural Science* **1982,** *38*, (FEB), 602-605.
38. Ahmed, I. A. M.; Young, S. D.; Mosselmans, J. F. W.; Crout, N. M. J.; Bailey, E. H., Coordination of Cd2+ ions in the internal pore system of zeolite-X: A combined EXAFS and isotopic exchange study. *Geochimica et Cosmochimica Acta* **2009,** *73*, (6), 1577-1587.
39. Lide, D. R., *CRC Handbook of Chemistry and Physics*. 88th ed.; CRC Press, Taylor & Francis Group: Boca Raton, USA, 2007.
40. Dang, L. X.; Schenter, G. K.; Fulton, J. L., EXAFS Spectra of the Dilute Solutions of Ca2+ and Sr2+ in Water and Methanol. *The Journal of Physical Chemistry B* **2003,** *107*, (50), 14119-14123.
41. Hasegawa, Y.; Hotta, H.; Sato, K.; Nagase, T.; Mizukami, F., Preparation of novel chabazite (CHA)-type zeolite layer on porous alpha-Al(2)O(3) tube using template-free solution. *Journal of Membrane Science* **2010,** *347*, (1-2), 193-196.
42. Mimura, H.; Kanno, T., Distribution and Fixation of Cesium and Strontium in Zeolite A and Chabazite. *Journal of Nuclear Science and Technology* **1985,** *22*, (4), 284-291.
43. Yang, S.; Navrotsky, A., An in situ calorimetric study of zeolite crystallization kinetics. *Microporous and Mesoporous Materials* **2002,** *52*, (2), 93-103.

Table 1 BET surface area measured in sediments reacted in YCW.

Sample	BET surface area ($m^2 g^{-1}$)
Unreacted	4.69 ± 0.01
10 day	1.46 ± 0.02
30 day	2.11 ± 0.31
90 day	1.49 ± 0.01
180 day	1.37 ± 0.01
365 day	1.66 ± 0.02
365 day + 70°C	5.45 ± 0.03

[TO BE PRINTED AT SINGLE COLUMN WIDTH]

Table 2 Sr K-edge EXAFS model fitting parameters where n is the occupancy (± 25%), r is the interatomic distance (± 0.02 Å for the first shell, ± 0.05 Å for outer shells),$2\sigma^2$ is the Debye-Waller factor (± 25%), and *R* is the least squares residual. *Fixed

Sample	**Shell**	**n**	**R (Å)**	**$2\sigma^2$ (Å^2)**	***R***
Sr^{2+} solution	O	9.1	2.58	0.031	26.3
$SrCO_3$	O	9*	2.64	0.027	20.3
	C	6*	3.04	0.032	
	Sr	6*	4.22	0.029	
	Sr	4*	4.97	0.033	
YCW 10 days	O	8.5	2.59	0.025	27.3
	Si(Al)	2.7	3.79	0.020	
YCW 365 days	O	7.8	2.60	0.024	21.8
	Si(Al)	1.2	3.84	0.018	
YCW 365 days + 70°C	O	8.2	2.67	0.027	32.9
	Si(Al)	5.5	3.45	0.028	

[TO BE PRINTED AT SINGLE COLUMN WIDTH]

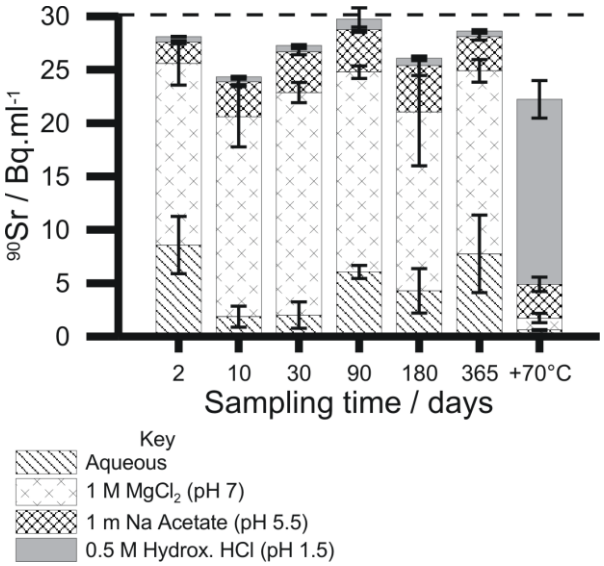

Figure 1 ^{90}Sr concentrations recovered in sequential extractions performed on sediments aged in young cement water solution. Dashed line at 30 Bq ml^{-1} equates to 100% recovery.

[TO BE PRINTED AT SINGLE COLUMN WIDTH]

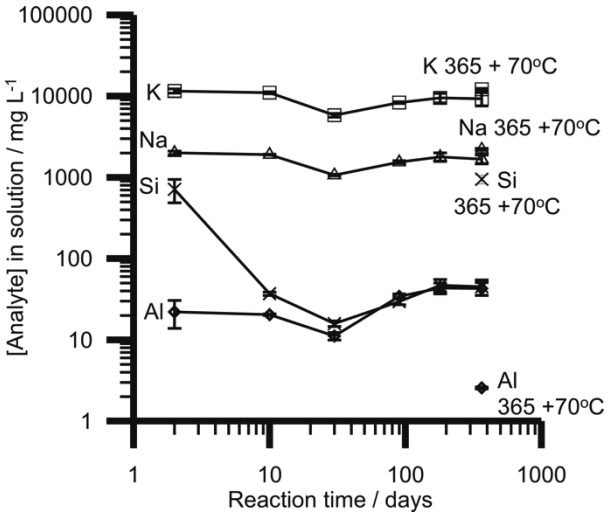

Figure 2 Concentration of selected major elements during the one year reaction of sediments with YCW.

[TO BE PRINTED AT SINGLE COLUMN WIDTH]

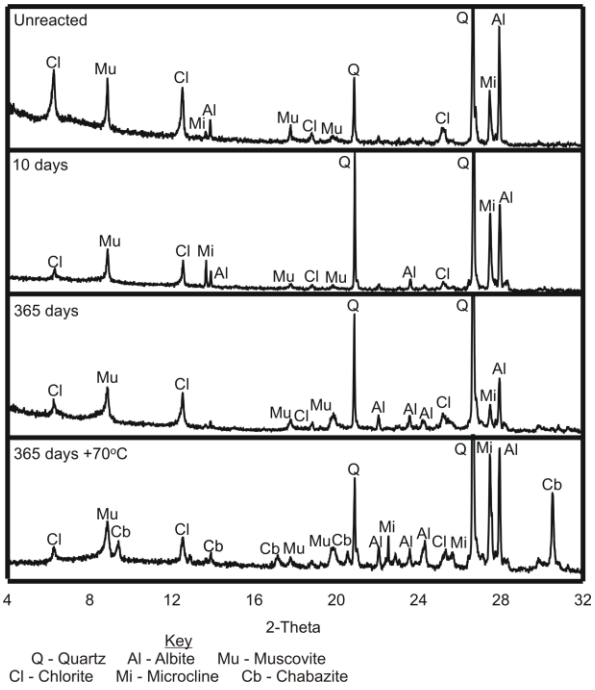

Figure 3 XRD patterns collected from fine fraction sediment samples at time points shown. Chlorite peaks are relatively more prominent in unreacted sediments, chabazite peaks only found for the sample incubated for 365 days +70 ^{o}C.

[TO BE PRINTED AT SINGLE COLUMN WIDTH]

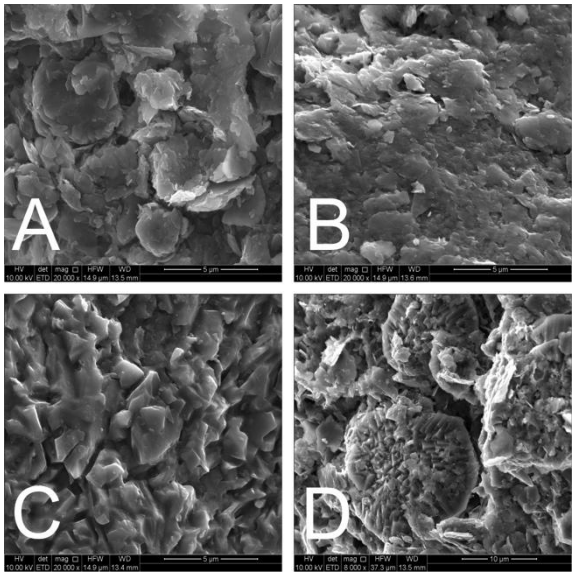

Figure 4 Scanning electron photomicrographs of sediment samples under the following conditions. A) Unreacted coarse sediment; B) after 10 day reaction in YCW; C) after 365 days reaction in YCW, and; D) after 365 days reaction at 70 ^{o}C.

[TO BE PRINTED AT SINGLE COLUMN WIDTH]

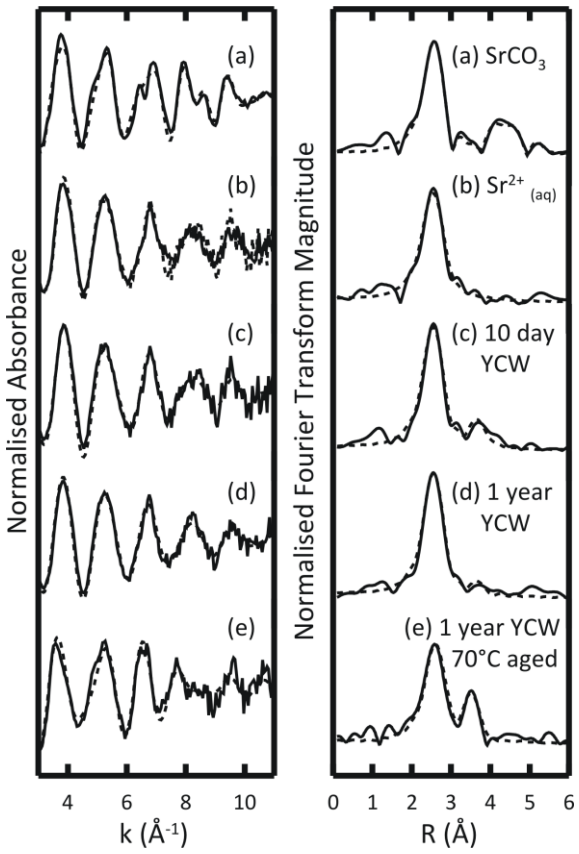

Figure 5 Background subtracted Sr K-edge EXAFS spectra (left hand side) and related Fourier transformations (right hand side) collected from (a) $SrCO_3$, (b) 3000 mg L^{-1} Sr^{2+} solution and (c-e) sediment samples aged with Sr^{2+} and YCW for 10 days, 365 days, or 365 days +70°C. Dashed line represent model fits produced in DLexcurv V1.0 using the parameters listed in Table 2.

[TO BE PRINTED AT SINGLE COLUMN WIDTH]